

IC/Microfluidic Hybrid System for Biology: Review

(Invited Paper)

Yong Liu, Hakho Lee, Robert M. Westervelt, and Donhee Ham
Harvard University, Cambridge, MA 02138

Abstract— This paper reviews our recent development of an integrated circuit (IC)/microfluidic hybrid system. The hybrid system consists of an IC chip and a microfluidic channel fabricated on top. Biological cells attached to magnetic beads are suspended inside the microfluidic system that maintains biocompatibility. A microcoil array in the IC produces programmable, spatially-patterned magnetic fields to simultaneously manipulate multiple individual bead-bound cells with precise position control. Two prototypes validate the proposed approach.

Keywords— Integrated circuits, microcoils, microfluidics, cell manipulations, biolab-on-IC, lab-on-a-chip.

I. INTRODUCTION

TODAY'S semiconductor integrated circuits (ICs) can contain over 100 million transistors, operate at GHz speeds, process Gbyte data, and can be manufactured inexpensively. With these advantages, the ICs have become one of the most significant enabling technologies of our time, lying at the heart of today's advanced computers and communication systems.

There has lately been a growing interest in exploiting the benefits of the ICs for biological applications. Bioanalytical instruments have been miniaturized on IC chips to study neural activities and tissue dynamics, to monitor ion channels, to probe DNAs, and to electrically manipulate cells [1] - [5]. These *biolab-on-IC* systems utilize the IC to facilitate faster, repeatable, and standardized biological experiments at low cost with a small volume of biological sample.

As a new biolab-on-IC, the authors have recently introduced an *IC/microfluidic hybrid system* that combines the biocompatibility of microfluidic systems with the programmability of IC chips [6] [7]. In this approach, a microfluidic system is placed on top of an IC and biological cells tagged by magnetic beads are suspended inside the microfluidic system. A microcoil array in the IC generates spatially-patterned magnetic fields. By dynamically changing the field pattern, the hybrid system can simultaneously manipulate many individual bead-bound-cells along different paths. Offering possibilities for biological and biomedical applications such as microscale tissue assembly [8], the hybrid system adds a new direction in the growing field of biolab-on-IC.

This work was supported by an IBM Faculty Partnership Award, NSF ITR Grant No. ECS-0313143, NSF Grant No. PHY-0117795, the NSF Nanoscale and Engineering Center (NSEC).

Donhee Ham and Yong Liu are with Electrical Engineering, Division of Engineering and Applied Sciences (DEAS), Harvard University. Hakho Lee is with Department of Physics at Harvard University. Robert M. Westervelt is with Department of Physics and DEAS, Harvard University.

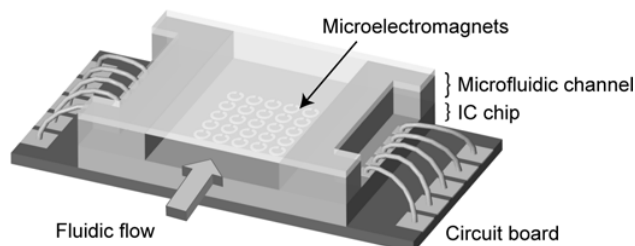


Fig. 1. Conceptual illustration of the IC/microfluidic hybrid system.

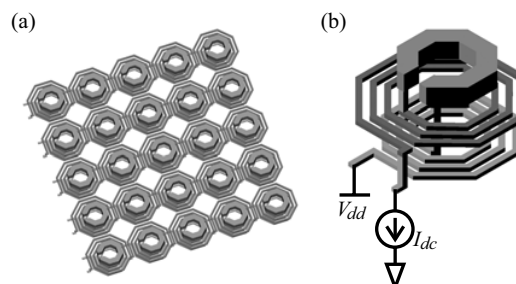


Fig. 2. (a) Microcoil array. (b) Microcoil with a current source.

This paper is the review of our IC/microfluidic hybrid system. Section II presents the basic concept of the hybrid technology. In Sections III and IV, we describe our two hybrid prototypes, which demonstrate the concept of the proposed system.

II. IC/MICROFLUIDIC HYBRID SYSTEM

A. Overview

The hybrid system consists of an IC and a microfluidic system fabricated on top of the IC as conceptually illustrated in Fig. 1. Biological cells attached to magnetic beads are suspended inside the microfluidic system where biocompatibility is maintained. The IC contains an array of microcoils (Fig. 2(a) shows an example.), which produces spatially-patterned magnetic fields on the surface of the IC. In a given magnetic field pattern, the bead-bound-cells are attracted towards local field peaks and trapped on the surface of the IC. Therefore, by modifying the spatial field pattern and hence by moving the field peak positions, the individual bead-bound-cells can be transported to their desired locations [8] [9]. The modification of the field pattern is done by changing the current distribution in the microcoil array using control electronics. For instance, each microcoil can be connected to its own current source for independent magnetic field control as depicted in Fig. 2(b).

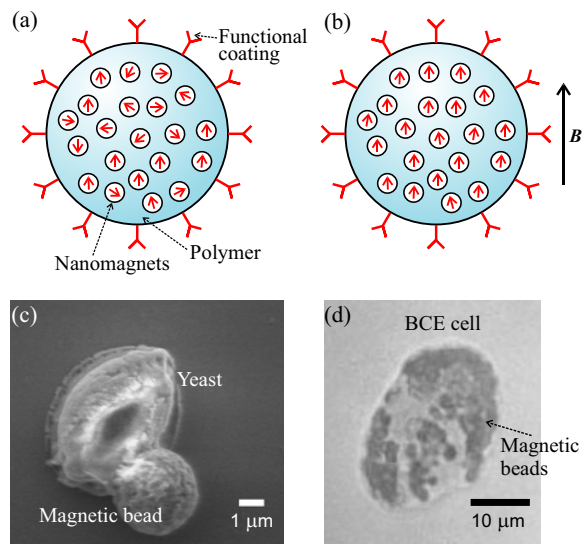


Fig. 3. (a) Structural schematic of a magnetic bead with $B = 0$. (b) Magnetic bead when $B > 0$. (c) A bead-bound yeast cell. (d) A BCE cell that has engulfed multiple beads.

Magnetic manipulation of bead-bound cells *per se* has been widely employed in biology [10]. However, in the conventional approach, a large group of bead-bound-cells are statistically pulled all at once using magnetic fields of low spatial resolution, *e.g.*, magnetic fields from magnetic tweezers. In contrast, one of the key aspects of our approach is the generation of microscopic magnetic field patterns using the microcoil array, which permits manipulation of many *individual* cells, moving each cell along a different path.

Because the spatial field patterns can be reconfigured by the IC, our hybrid system offers more flexibility in cell manipulation over the conventional microfluidic system. The conventional microfluidic system moves biological samples in a fixed channel network using predetermined valve controls, and hence, different operations require different specific microfluidic systems. In contrast, the hybrid system can perform various and sophisticated cell manipulation operations not by necessarily requiring a change in the microfluidic system structure, but by reconfiguring the spatial pattern of the magnetic fields. In this sense the hybrid system is a *programmable microfluidic system*.

Our cell manipulation method is a magnetic counterpart of the electric cell manipulation scheme utilizing dielectrophoresis (DEP) [5]. Each approach has its own advantages and disadvantages. For example, while the magnetic method requires more sample preparation efforts (magnetic bead attachment), it is more biocompatible as magnetic fields are transparent to cells. Depending on specific experimental needs, a proper choice should be made between the two technologies, for optimum manipulation operation.

B. Magnetic Beads and Bead-Bound-Cells

Attaching magnetic beads to cells is a well-established technique from the conventional low-resolution magnetic

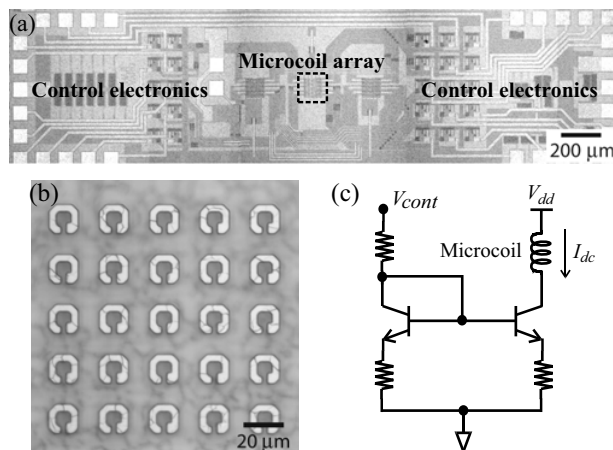


Fig. 4. (a) Micrograph of the SiGe IC (4 mm \times 1 mm). (b) Microcoil array close-up. (c) Control electronics for a single microcoil.

manipulation approach [10]. As this procedure is essential in our approach as well, we briefly explain the technique here as a background. The magnetic bead is a polymer microsphere containing a large number of nanomagnets as shown in Figs. 3(a) and (b). In the absence of an external magnetic field, the magnetic moments of the nanomagnets are randomly oriented due to thermal agitations [Fig. 3(a)], and hence, the bead has no net magnetic moment. In the presence of an external magnetic field, however, the magnetic moments of the nanomagnets line up overcoming the thermal fluctuations, and the magnetic bead will exhibit an appreciable net magnetic moment as illustrated in Fig. 3(b). It is this magnetic moment that interacts with the magnetic field pattern in the manipulation process.

To attach the magnetic bead to a cell, the surface of the magnetic bead is coated with specific proteins. This functionalized-bead then can be bound to specific target cells. Figure 3(c) shows an example, a yeast cell attached to a micron-scale magnetic bead. Figure 3(d) shows another example where 30 \sim 50 magnetic beads of diameter 250 nm are even engulfed by a bovine capillary endothelial (BCE) cell. Magnetic beads have been known to be biocompatible: many different types of cells attached to them can grow and live normally [10].

III. SiGe IC/MICROFLUIDIC HYBRID PROTOTYPE

This section describes our first hybrid prototype utilizing a SiGe IC. This first prototype is used to demonstrate the basic concept of the proposed approach [6].

A. SiGe IC

Figure 4(a) is a die micrograph of the IC fabricated in ADI's SiGe bipolar technology. This IC incorporates an array of 5 \times 5 microcoils [Fig. 4(b)]. Using EM simulations, each microcoil is designed to create a single magnetic field peak on the chip surface when a current is drawn [6] [8]. Each microcoil is connected to its own current source-mirror pair [Fig. 4(c)] for an independent current control.

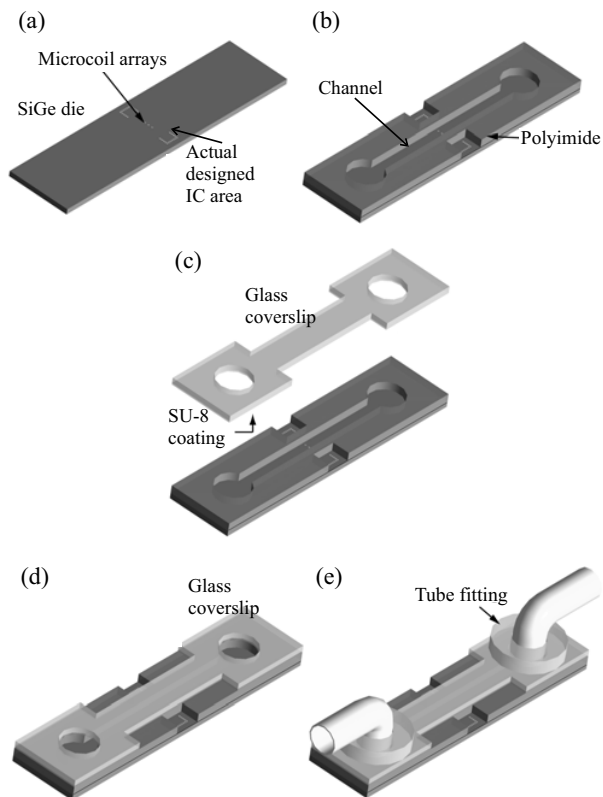


Fig. 5. Post-fabrication of the microfluidic system to construct our first hybrid prototype.

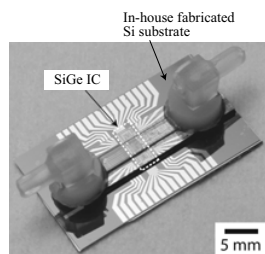


Fig. 6. Photo of the first hybrid prototype.

B. SiGe IC/Microfluidic Hybrid Prototype

To construct the hybrid system, a microfluidic system is post-fabricated on top of the SiGe IC. Figure 5 shows the sequence of the post-fabrication steps. First, the IC is diced from the wafer [Fig. 5(a)], where the diced area is larger than the designed IC area. This extra area is used as a platform on which a microfluidic system is fabricated. Second, polyimide is spin-coated and patterned on the surface of the SiGe die to form sidewalls of a microfluidic channel [Fig. 5(b)]. The channel height and width are 30 and 1000 μm , respectively. Third, a glass coverslip is sealed on top of the channel sidewalls [Figs. 5(c) and (d)] using a negative photoresist as a sealing agent. Finally, fluidic tube fittings separately fabricated are glued to the inlet and outlet of the microfluidic system [Fig. 5(e)].

Figure 6 is the photo of the completed SiGe IC/microfluidic hybrid system, which sits on top of an in-house fabricated silicon substrate that contains electrical

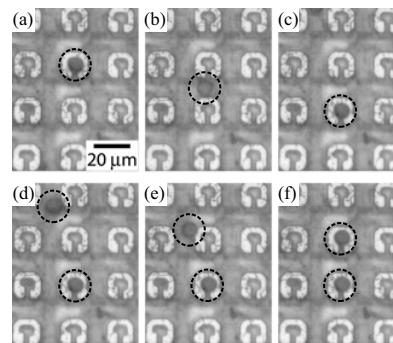


Fig. 7. Manipulation of individual beads with the first prototype.

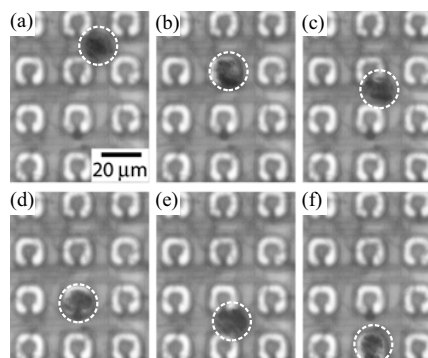


Fig. 8. Manipulation of a BCE cell that has engulfed multiple beads.

leads. This substrate facilitates handling and electrical interconnections. To prevent electromigration of the chip and to keep the system temperature at biocompatible 37 $^{\circ}\text{C}$, the whole system was mounted on a copper stage whose temperature was regulated by a thermoelectric cooler.

C. Experimental Results

To demonstrate the manipulation capabilities of the first hybrid prototype, two different objects, magnetic beads and BCE cells that has engulfed multiple magnetic beads [Fig. 3(d)], are used as target samples.

The sequence of the micrographs in Fig. 7 shows manipulation of individual magnetic beads using the hybrid system. Magnetic beads of diameter 8.5 μm and magnetic susceptibility 0.2 are suspended in distilled water in the microfluidic channel. By activating a microcoil with a current of 11 mA, a single magnetic bead is trapped at the center of the coil (Image a). The magnitude of the magnetic field peak is 15 G and trapping force is 20 pN. By deactivating the microcoil and simultaneously activating an adjacent coil, the bead is moved to the adjacent coil with an average speed of 1 $\mu\text{m}/\text{s}$ (Images b and c). While the magnetic bead is trapped, another magnetic bead is trapped by creating an additional field peak within the coil array (Images d to f). Repeating the same protocol, a larger number of beads can be manipulated independently and simultaneously.

The sequence of the micrographs in Fig. 8 shows the trapping and translation of a single BCE cell using the hybrid system. A single magnetic peak of 15 G is created

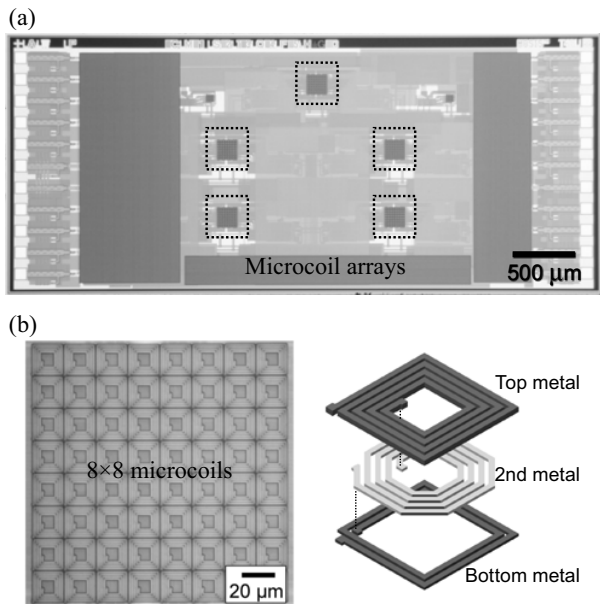


Fig. 9. (a) CMOS IC (5 mm \times 2 mm). (b) The microcoil array close-up and the structure of a microcoil in the array.

in a microcoil, trapping a single cell with a force of 50 pN (Images a and b). Subsequently by moving the field peak position, the trapped cell is moved to adjacent coils with an average speed of 6 $\mu\text{m/s}$ (Images c to f). The BCE cell remains viable during and after the experiments, indicating the non-invasiveness of the manipulation process.

IV. CMOS IC/MICROFLUIDIC HYBRID PROTOTYPE

In this section, we describe the development and operation of our second hybrid prototype implemented with a CMOS IC. Based on the experimental results from the first hybrid prototype, the IC chip was redesigned to enhance cell manipulation capabilities. First of all, the number of microcoils in the array was increased to handle a larger number of cells. With this capability, the second prototype can be used, for example, to assemble a 2-dimensional (2D) artificial biological tissue at the microscale. The assembled tissue can be used to study intercellular communications, one of the fundamental questions in cell biology [12]. To facilitate the operation of the large microcoil array, digital logic and timing circuits are integrated in the same chip, taking full advantage of CMOS technology.

Figure 9(a) shows a die micrograph of the CMOS chip. The chip is fabricated in TSMC 0.18 μm technology and measures 5 mm \times 2 mm. The chip contains five 8 \times 8 microcoil arrays. Figure 9(b) shows the close-up of one of the arrays along with the structure of the microcoil in the array. The outer diameter of the microcoil is 20 μm , and three metal layers are used to form the microcoil. As in the first hybrid prototype, the microcoil is designed to produce a single magnetic field peak at its center on the chip surface.

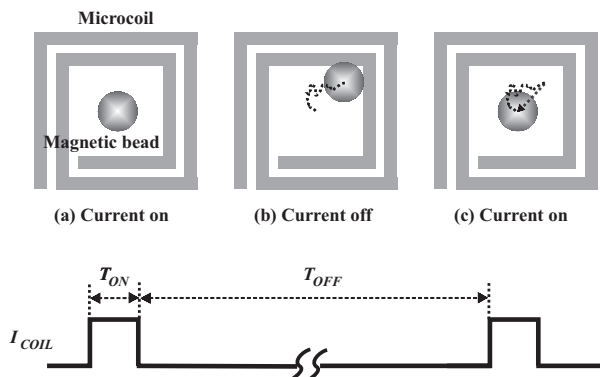


Fig. 10. Basic idea behind the low power operation.

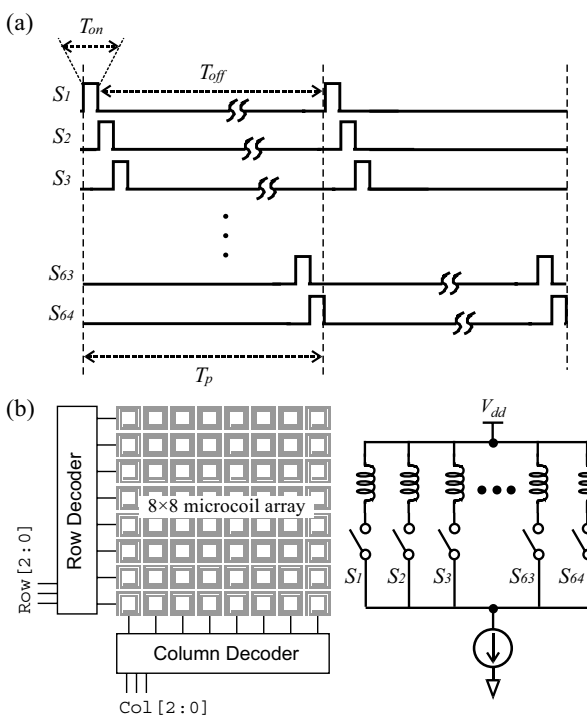


Fig. 11. (a) Low power current distribution signaling among the 64 microcoils ($N = 8$). (b) Simplified schematic for the 8 \times 8 microcoil array control electronics.

A. Low Power Operation of the Large Microcoil Array

The most straightforward protocol to control the current distribution in an $N \times N$ microcoil array to trap and manipulate individual cells is to implement N^2 separate on-chip current sources, one for each microcoil, and to switch on and off the current sources independently. This protocol which was employed in the first prototype, however, faces a severe power dissipation problem as the number of microcoils increases as is the case of the second prototype. For instance, when assembling a biological tissue using this current distribution scheme, all of the N^2 microcoils need to remain on in order to maintain trap of N^2 cells, one cell for each microcoil. This leads to a prohibitively large power dissipation, which can cause thermal failure of the chip and damage to the cells through heat shock.

To address this issue, we developed a new current distribution protocol, which exploits the fact that CMOS electronics is far faster than the motion of microscale objects in microfluid. Figure 10 illustrates the basic idea behind the new protocol using one microcoil first. To maintain a trap of a magnetic bead within the microcoil, instead of drawing a continuous current flow, the microcoil draws a current for a time duration of T_{on} and is then deactivated to remain off for the next time duration of T_{off} . This two-step procedure completed in the period of $T_p = T_{on} + T_{off}$ is repeated. During the on-time T_{on} , the magnetic bead remains trapped at the center of the microcoil [Fig. 10(a)]. Once the microcoil is turned off, the initially-trapped bead undergoes the Brownian motion, walking away from the center of the microcoil [Fig. 10(b)] during the off-time duration, T_{off} . However, the microcoil is activated again to repeat the two-step procedure before the bead completely escapes the microcoil, hence trapping the bead back to the center of the microcoil [Fig. 10(c)]. Therefore with this protocol, the magnetic bead can remain trapped without necessarily supplying a continuous current to the microcoil.

To attain a low power operation of the $N \times N$ microcoil array, the procedure described above is sequentially applied to all the microcoils in the array. Each microcoil is turned on once for T_{on} during one period, $T_p = N^2 \cdot T_{on}$, as illustrated in Fig. 11(a) [$N = 8$]. This period (T_p) is repeated, and during one period, only one microcoil is activated at any given moment. As far as the off-time, $T_{off} = (N^2 - 1) \cdot T_{on}$, of each microcoil is shorter than the characteristic diffusion time constant due to the Brownian motion, the microcoil array can maintain traps of up to N^2 cells (one cell for each microcoil) sharing a common current source at different times, allowing a low power operation. The period T_p can assume a wide range of values depending on the hydrodynamic properties of the cells and the size of the microcoils. However, the characteristic speeds of the cells in microfluid are far smaller than the GHz speed CMOS electronics, and therefore, the proposed timing scheme is easily achievable with the CMOS IC.

Figure 11(b) shows the simplified schematic of the microcoil array circuit to realize the low-power protocol. Each microcoil in the array is connected to a common current source through a FET switch. The switches are clocked according to the current distribution protocol using the command signals coming from the row and column decoders.

B. CMOS IC/Microfluidic Hybrid Prototype

To construct the second hybrid prototype, a microfluidic channel is post-fabricated on top of the CMOS IC. The fabrication procedure is modified from that for the first hybrid prototype to make fluidic connections through the backside of the device. Figure 12 shows the sequence of the post-fabrication steps. First, the CMOS IC chip is glued onto an in-house fabricated silicon substrate that contains lithographically-patterned electrical leads [Fig. 12(a)]. The substrate facilitates electrical interconnections and also serves as a platform on which a microfluidic system is fabricated. Second, a negative photoresist (SU-8) layer with

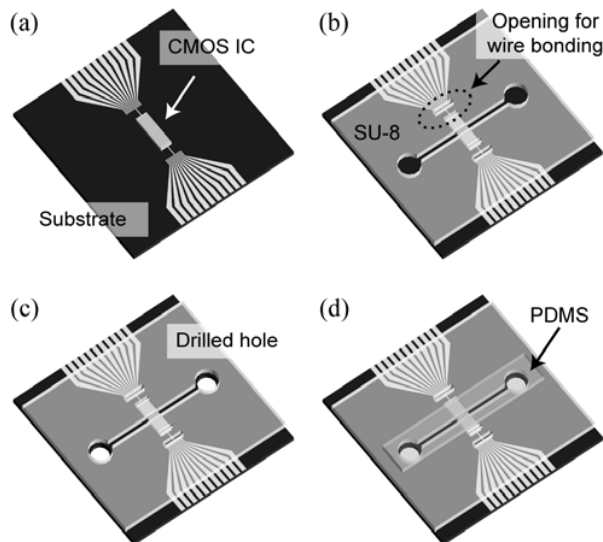


Fig. 12. Fabrication process to implement a microfluidic system on top of the CMOS IC.

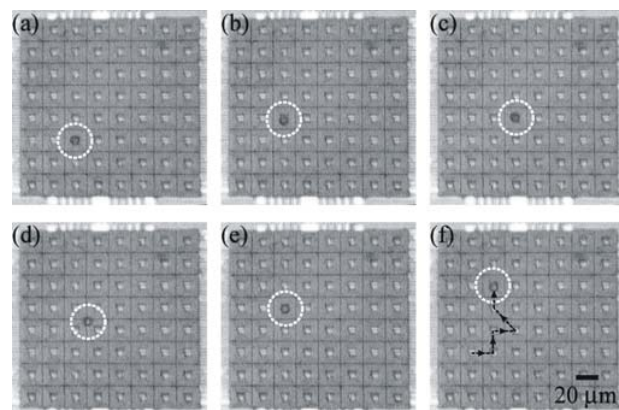


Fig. 13. Manipulation of a single magnetic bead using the CMOS IC/microfluidic hybrid prototype.

thickness $\sim 350 \mu\text{m}$ is spin-coated on the substrate. The SU-8 layer is then lithographically patterned to define the sidewalls of a microfluidic channel and to open up pad areas for wire bonding [Fig. 12(b)]. After patterning the SU-8 structure, two holes are drilled on the substrate to form microfluidic ports [Fig. 12(c)]. A PDMS layer of $\sim 500 \mu\text{m}$ thickness is prepared by cast-coating and cured [11]. The cured PDMS layer is cut into a desired shape and placed on top of the SU-8 structure to seal the microfluidic channel.

C. Experimental Results

Magnetic beads are used to demonstrate the capabilities of the second hybrid prototype. Magnetic beads of diameter $8.5 \mu\text{m}$ and magnetic susceptibility 0.2 are suspended inside the microfluidic channel.

Figure 13 shows the manipulation of a single magnetic bead. By activating a microcoil with a dc current of 20 mA, a magnetic field peak ($B = 30 \text{ G}$) is produced, trapping the bead at the coil center with the force of $\sim 40 \text{ pN}$ [Fig. 13(a)]. After the initial trap, the bead is moved to an adjacent microcoil by moving the field peak [Fig. 13(b)].

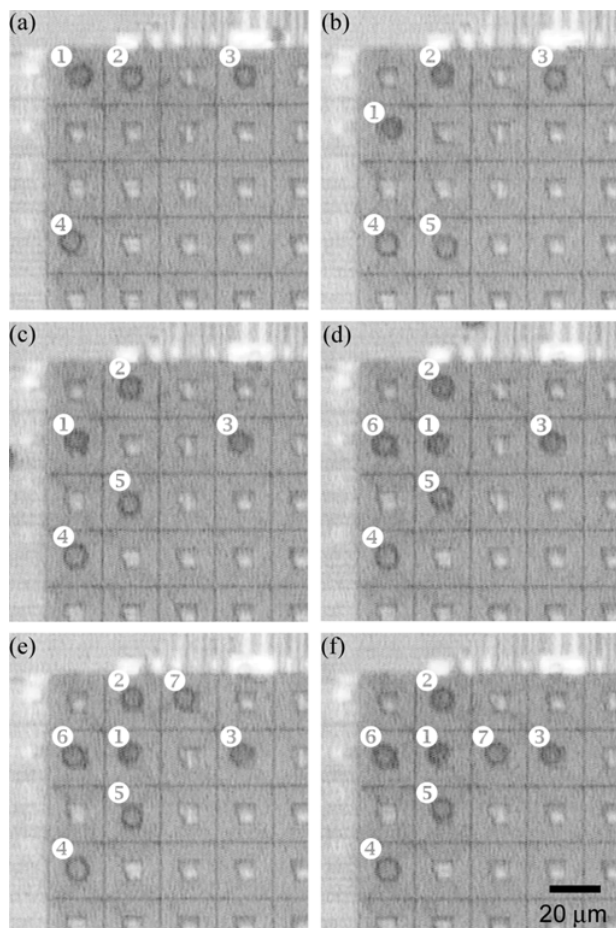


Fig. 14. Manipulation of multiple magnetic beads using the CMOS IC/microfluidic hybrid prototype.

Repeating this procedure [Fig. 13(c) to (e)], the bead is transported over a distance of $100\ \mu\text{m}$ with the average speed of $11\ \mu\text{m/s}$. Fig. 13(f) shows the overall path.

The low-power current distribution scheme is verified by manipulating up to seven magnetic beads simultaneously [Fig. 14]. Every microcoil in the 8×8 array is sequentially activated with $T_{on} = 10\ \text{ms}$, while sharing the same dc current of $20\ \text{mA}$ to trap or release a magnetic bead. Initially four magnetic beads, one bead at one microcoil, are trapped [Figs. 14(a)] by generating four magnetic peaks [$B = 30\ \text{G}$]. While rearranging the four beads, another magnetic bead is trapped and moved [Figs. 14(b) and (c)]. This process is repeated to eventually arrange six magnetic beads in a cross shape [Figs. 14(d) to (f)]. This experiment clearly verifies the low-power operation to simultaneously manipulate individual magnetic beads.

V. CONCLUSION

In this paper we reviewed our recent development of an IC/microfluidic hybrid system. The unique coupling of the programmability of the IC and the biocompatibility of the microfluidic system allows simultaneous manipulation of many individual magnetic beads and bead-bound biological cells with easy and precise control. The hybrid system is a

miniaturized, self-contained system that integrates control electronics. Due to the low fabrication cost, the hybrid system can be used as a single-use, disposable device.

The IC/microfluidic hybrid system offers an interesting direction in the field of lab-on-a-chip with prospect of enabling important biological applications. One significant potential application is to assemble a 2D biological tissue at the microscale. By bringing cells one by one with precise spatial control, the hybrid system can build an artificial tissue in a standardized and repeatable manner with tight demographic quality control measures. The assembled tissue can be used as a model tissue to study communications between different types of cells or to test drug efficacy.

There still remain challenges to further mature the hybrid technology. The most important task is to perfect the long-term biocompatibility. To this end, investigations of proper chip surface treatments and on-chip temperature regulators should be made. Another interesting direction is to develop an all-electrical on-chip sensor (for each microcoil) that can map the distribution of magnetic beads. Such sensors will render bulky optics unnecessary, realizing a true lab-on-a-chip.

VI. ACKNOWLEDGEMENT

The authors would like to thank Larry DeVito and Susan Feindt of Analog Devices for their continued support and chip fabrications. The authors acknowledge Kevin Kit Parker at Harvard for discussions. Donald Ingber at Harvard Medical School provided the BCE cells. AnSoft and Sonnet donated their field solvers.

REFERENCES

- [1] P. Eversmann *et al*, "A 128×128 bio-sensor array for extracellular recording of neural activity," *ISSCC Dig. Tech. Papers*, pp. 222-223, Feb., 2003.
- [2] R. A. Kaul *et al*, "Neuron-semiconductor chip with chemical synapse between identified neurons," *Phys. Rev.* vol. 92, no. 3, pp. 38102/1-38102/4, Jan., 2004.
- [3] P. Fromherz, "Joining ionics and electronics: semiconductor chips with ion channels, nerve cells, and brain tissue," *ISSCC Dig. Tech. Papers*, pp. 76 - 77, Feb., 2005.
- [4] P. Cailat *et al*, "Active CMOS biochips: an electro-addressed DNA probe," *ISSCC Dig. Tech. Papers*, pp. 272-273, Feb. 1998.
- [5] N. Manaresi *et. al.*, "A CMOS chip for individual cell manipulation and detection," *IEEE Journal of Solid-State Circuits*, vol. 38, no. 12, pp. 2297 - 2305, 2003.
- [6] H. Lee, Y. Liu, E. Alsberg, D. E. Ingber, R. M. Westervelt, and D. Ham, "An IC/Microfluidic hybrid microsystem for 2D magnetic manipulation of individual biological cells," *ISSCC Dig. Tech. Papers*, pp. 80 - 81, Feb, 2005.
- [7] H. Lee, Y. Liu, R. M. Westervelt, and D. Ham, "A CMOS/Microfluidic hybrid microsystem for 2D magnetic manipulation of individual biological cells," Submitted to *IEEE Journal of Solid-State Circuits*.
- [8] H. Lee, *Microelectronic / microfluidic hybrid system for the manipulation of biological cells*, PhD dissertation, Harvard University, 2005.
- [9] H. Lee, A. M. Purdon, and R. M. Westervelt, "Manipulation of biological cells using a microelectromagnet matrix," *Applied Physics Letters*, vol. 85, pp. 1063 - 1065, 2004.
- [10] U. Hafeli, *Scientific and clinical applications of magnetic carriers*, Plenum press, New York, 1997.
- [11] G. M. Whitesides *et al*, "Soft lithography in biology and biochemistry," *Annu. Rev. Biomed. Eng.*, vol. 3, pp. 335, 2001.
- [12] S. N. Bhatia *et al*, "Tissue engineering at the microscale," *Biomed. Microdevices*, vol. 2, pp. 131-144, 1999.